

A peer-reviewed open-access journal indexed in NepJol

ISSN 2990-7640 (online); ISSN 2542-2596 (print)

Published by Molung Foundation, Kathmandu, Nepal

Article History: Received on Nov 1, 2024; Accepted on Dec 27, 2024

DOI: <https://doi.org/10.3126/mef.v15i01.74027>

**Remarkable Photocatalytic and Antimicrobial Activities of Iron Oxide Nanoparticles Synthesized through Green Route Using *Citrus maxima* Peel Extract**

Kamal Prasad Sapkota<sup>1,2</sup>, Bijay Kumar Das,<sup>2</sup> and Motee Lal Sharma<sup>1</sup>

<sup>1</sup>Central Department of Chemistry, Institute of Science and Technology,  
Tribhuvan University

<sup>2</sup>Department of Chemistry, Amrit Campus

**Author Note**

Kamal Prasad Sapkota, Ph.D.  <https://orcid.org/0000-0002-0452-7796> is an Assistant Professor at the Central Department of Chemistry, Institute of Science and Technology, Tribhuvan University, Kirtipur, Kathmandu, Nepal. He specializes in Materials Chemistry, Nanocomposites, Photocatalytic Water Splitting, Photocatalysis, Bactericidal Activities and Anticancer Activities.

Bijay Kumar Das  <https://orcid.org/0009-0003-2059-9970> has a Master of Science in Chemistry from Amrit Campus, Tribhuvan University. He teaches at Shree Janta Rastriya Madhyamik Vidhyalaya, Dhamaura, Mahottari, Madhesh Province, Nepal.

Motee Lal Sharma, Ph.D.  <https://orcid.org/0000-0003-2564-0912> is a Professor at the Central Department of Chemistry, Institute of Science and Technology, Tribhuvan University, Kirtipur, Kathmandu, Nepal. He specializes in Materials Chemistry, Coordination Chemistry, Supramolecular Chemistry, and Docking studies.

The authors declare no conflict of interest.

This research was partially funded by Amrit Campus, Tribhuvan University.

Correspondence concerning this article should be addressed to Kamal Prasad Sapkota, Central Department of Chemistry, Institute of Science and Technology, Tribhuvan University, Kirtipur, Kathmandu, Nepal. Email: [kamal.sapkota@cdc.tu.edu.np](mailto:kamal.sapkota@cdc.tu.edu.np) / [mychemistry2037@gmail.com](mailto:mychemistry2037@gmail.com)

### Abstract

The present research work reports the successful synthesis of the iron oxide nanoparticles (IONPs) through green route, their characterization and their application for their antimicrobial and photocatalytic performance. The IONPs were prepared using *Citrus maxima* peel extract through green synthesis method. The peel extract was found to contain important phytochemicals such as polyphenols, flavonoids, and terpenoids, which facilitate the reduction of metal precursors and stabilize metal nanoparticles. This approach offers scalability, simplicity, and non-toxicity, making it a notable strategy in green nanotechnology for producing nanoparticles. The as-synthesized nanoparticles were applied for the antimicrobial and photocatalytic performance. It was found that the as-synthesized IONPs were excellent photocatalysts for the degradation of methylene blue solution with 98.13% degradation within the recorded time of 90 minutes in the presence of natural sunlight. Moreover, the IONPs demonstrated good anti-bacterial activity against *Bacillus subtilis* and *E. coli* and good anti-fungal activity against *Candida albicans*.

*Keywords:* Iron oxide nanoparticles, green synthesis, *Citrus maxima* peel extract, antimicrobial activity, photocatalytic activity

### **Remarkable Photocatalytic and Antimicrobial Activities of Iron Oxide Nanoparticles Synthesized through Green Route Using *Citrus maxima* Peel Extract**

Nanotechnology focuses on creating and assembling materials at the scale of 1-100 nm (Adhikari et al., 2022). Metal nanoparticles are widely studied due to their unique physicochemical properties, including electronic, magnetic, catalytic, and antimicrobial activities. The field is advancing rapidly, with applications in catalysis, agriculture, electronics, and biomedical analysis (Caldeirao et al., 2021).

There are two main methods for nanoparticle synthesis: the top-down approach, which breaks down larger structures, and the bottom-up approach, where materials are built from atomic levels. Various chemical and biological methods are used for synthesis, with green synthesis emerging as an eco-friendly alternative that avoids toxic agents. Green synthesis uses biological materials like plants, bacteria, and fungi, which contain compounds that act as reducing and stabilizing agents in nanoparticle formation (Bhuiyan et al., 2020).

Carbon-based nanoparticles, such as fullerenes and carbon nanotubes, are valued for their electrical conductivity and structural properties. Fullerenes are globular, while nanotubes are tubular, and both are produced using processes like chemical vapor deposition. Green synthesis is seen as cost-effective, simple, and environmentally friendly, offering a sustainable approach to nanoparticle production without harmful by-products (Kumar et al., 2020; Sapkota et al., 2019).

Researchers are exploring plant extracts and other biomaterials to synthesize nanoparticles more sustainably. Plant-derived phytochemicals act as natural agents in nanoparticle formation, making green synthesis scalable and less toxic compared to conventional methods (Anchan et al., 2019).

#### **Iron Oxide Nanoparticles**

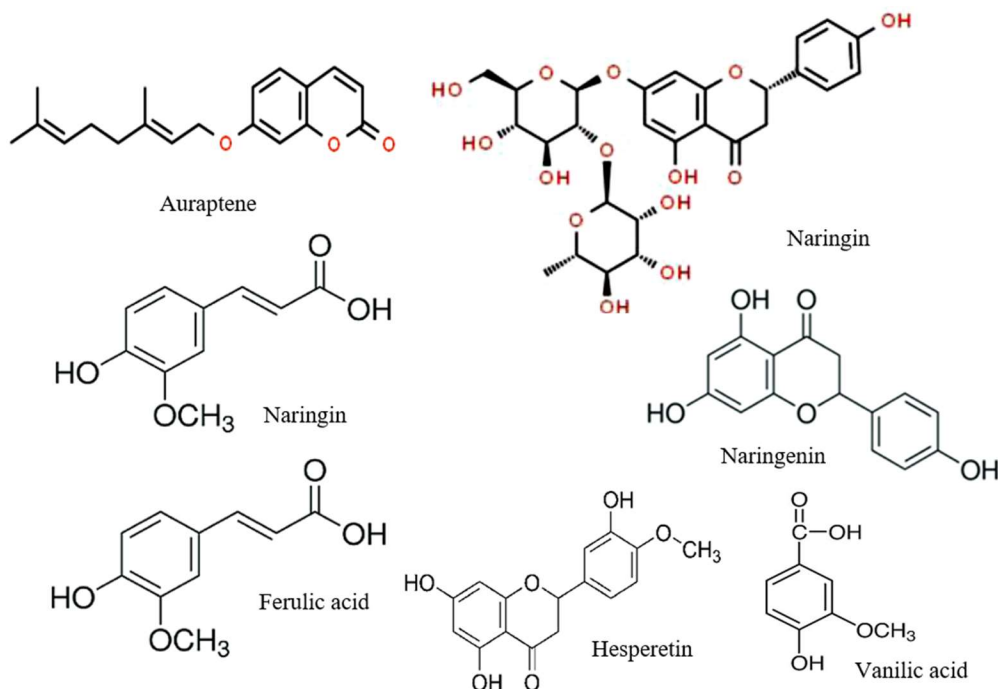
Iron oxide nanoparticles (IONPs) occur naturally and can be synthesized chemically for use in fields such as electronics, biomedicine, and environmental remediation. Hematite, maghemite, and magnetite are the most commonly studied iron oxides. Hematite is stable and has anti-ferromagnetic properties, making it useful in gas sensors and photocatalysts. Maghemite and magnetite are primarily employed in drug delivery and energy storage (Adhikari et al., 2022; Bibi et al., 2019).

Conventional synthesis methods like sol-gel, chemical vapor deposition, and pyrolysis involve toxic solvents and high temperatures, which can degrade magnetic properties. Using biological materials, green synthesis offers a cost-effective and eco-friendly alternative for producing iron oxide nanoparticles with desirable properties for biomedical and industrial applications. In this context, a greener, bottom-up method was used to create uniformly distributed spherical IONPs (Izadiyan et al., 2020; Kirdat et al., 2021).

The pomelo (*Citrus maxima*), a Southeast Asian fruit, is known for its nutritional and medicinal benefits. It boosts the immune system, helps regulate blood sugar, and has anti-aging properties. Different parts of the pomelo offer various health benefits, such as using the leaves to treat swelling, the seeds for coughs, and the fruit as a cardiogenic and digestive aid.

### **Figure 1**

*Some Phytochemicals Present in Citrus maxima Peel Extract (Zou et al., 2016)*



According to reports, *Citrus maxima* peel extract contains significant amounts of phenolic acids, coumarin flavonoids, rutin, and terpenoids (Figure 1). These substances are regarded as organic antioxidants. Furthermore, they can likewise function well as a reducing agent to create IONPs. Thus, IONPs were produced from this method are more biocompatible and appropriate for industrial and biomedical uses. Plant components (such as leaves, fruits, seeds, and bark) include various antibacterial components, such as antioxidants, phenolic substances, alkaloids, flavonoids, steroids, terpenoids, etc which is utilized for treatment (Yu *et al.*, 2016). Fresh pomelo fruit is eaten, whereas its peel is thrown away as biological waste. However, pomelo peel, which can make up to 30% of the fruit's weight, is regarded as a good source of important phytochemicals like pectin, cellulose, pectinoids, and essential oils. Pomelo peel extract contains flavonoids that can convert  $\text{Fe}^{3+}$  ions into metallic  $\text{Fe}(0)$  nanoparticles and additional use of other phytochemicals is possible to create films that are antibacterial and antioxidant used in medicine or food packaging.

It is hypothesized that iron oxide nanoparticles (IONPs) can be synthesized using *C. maxima* peel extract and these synthesized nanoparticles can be utilized for the photocatalytic degradation of organic dyes and it can also be employed for anti-microbial applications. However, there are still limited researches and comprehensive data on the biosynthetic process of synthesizing IONPs using *C. maxima* peel extract are not available. Moreover, limited applications have been explored. Some experiments have reported the synthesis of IONPs using *C. maxima* peel extract with applications in biomedical fields, catalysis, water purification, photocatalytic degradation of organic dyes and hazardous metal detection. However, detailed reports on the multiple applications of IONPs are still in high demand. Therefore, this research project will primarily focus on the synthesis of IONPs using *C. maxima* peel extract and their subsequent use in anti-microbial applications and photocatalytic degradation of dyes with the aid of a UV-visible spectrophotometer.

### **Materials and Methods**

The research was conducted entirely through laboratory experiments, and the data obtained were analyzed using various spectroscopic techniques. The research followed a systematic approach based on objectivity, generality, and verifiability, relying on the experimental results.

#### **Solvents and Chemicals**

The chemicals and solvents used in this research work include Ferric chloride hexahydrate ( $\text{FeCl}_3 \cdot 6\text{H}_2\text{O}$ ) from Fisher Scientific, ethanol, distilled water, Whatman filter paper (No. 40), NaOH, and 30%  $\text{H}_2\text{O}_2$  from Fisher Scientific. All these materials were obtained from the chemistry laboratory without further purification.

#### **Plant Extract Preparation**

*C. maxima* fruits were bought from the local market in Kathmandu. The fruits were washed with tap water and then with distilled water. Then, the peel was removed from fruit with the help of a knife and left for drying in sunlight for 7 days. The dried peels were ground to make a powder using an electrical blender and the remaining peels were stored in a polythene bag for future use. About 20 grams of the fine powder sample was heated in 600 mL of distilled water on a magnetic stirrer hot plate at 80°C for 30 minutes. The mixture was then filtered through Whatman Filter Paper after cooling and the collected filtrate was finally referred to as *C. maxima* peel extract. The extract was used for the experiments and the remaining extract was stored at 4°C in the refrigerator for further use.

#### **Preparation of Ferric Chloride Hexahydrate (Iron Chloride) Solution**

To maintain a 0.1M concentration of iron chloride solution, 6.8 grams of  $\text{FeCl}_3 \cdot 6\text{H}_2\text{O}$  were dissolved in 250 mL of distilled water. The resulting solution was then stored in a dark place away from sunlight.

#### **Green Synthesis of Iron Oxide Nanoparticles**

In the biosynthesis process, 50 mL of *C. maxima* peel extract was slowly added drop by drop to 50 mL of  $\text{FeCl}_3 \cdot 6\text{H}_2\text{O}$  in a 1:1 molar ratio at a temperature of 80°C on a magnetic stirrer hot plate. The mixture was stirred for one hour on a magnetic stirrer at a constant speed of 850 rotations per minute. The formation of a black-colored solution confirmed the synthesis of iron oxide nanoparticles (IONPs) as the color change was attributed to the surface plasmon resonance (SPR) effect and the conversion of  $\text{Fe}^{+3}$  ions to  $\text{Fe}_2\text{O}_3$  NPs by the aqueous *C. maxima* peel extract. The initial yellow color was mainly due to the *C. maxima* peel extract which gradually faded away and turned black as the concentration of IONPs increased. Subsequently, 1M NaOH was added to the reaction mixture until the pH reached 11, as measured by a pH meter. The formation of nanoparticles was confirmed using a UV-visible spectrophotometer which exhibited a characteristic maximum peak at a wavelength of 368 nm. The

synthesized IONPs were then stored in the refrigerator for further uses in separation, purification and characterization.

### **Purification and Separation of Iron Oxide Nanoparticles**

The synthesized IONPs were separated and purified through centrifugation at 8000 rpm for 10 minutes. The resulting pellet was washed 2-3 times with distilled water and then with ethanol to remove impurities. Finally, the nanoparticles were dried in a hot air oven at 80°C for 24 hours before being stored in a sealed container for subsequent characterization and applications.

### **Characterization of IONPs**

Characterizing IONPs is a crucial step in identifying and understanding the properties of the nanoparticles. Various analytical techniques were employed to determine the nanoparticles' size, shape, structure, morphology, surface chemistry, surface charge, surface area, and disparity. UV-visible spectroscopy was employed to affirm the formation of IONPs from the precursor. Fourier Transform Infrared (FTIR) spectroscopy was used to confirm the presence of different functional groups attached to IONPs that were derived from phytochemicals. X-ray diffraction (XRD) analysis was employed for the study of phase structure and crystallinity of the as-synthesized nanoparticles.

## **Results and Discussions**

The formation of IONPs was confirmed through the UV-vis spectroscopic analysis, FTIR spectroscopy and X-ray diffractometric analysis.

### **Formation of Iron Oxide ( $\alpha$ -Fe<sub>2</sub>O<sub>3</sub>) Nanoparticles**

The addition of 50 mL of *C. maxima* peel extract to a 50 mL solution of 0.1M FeCl<sub>3</sub>.6H<sub>2</sub>O in a 1:1 ratio resulted in the formation of IONPs, as evidenced by the change in color from brown to a darker shade. Such color change is attributed to the surface plasmon resonance (SPR) phenomenon typically observed in iron oxide nanoparticles and the conversion of Fe<sup>+3</sup> ions to Fe<sup>0</sup> nanoparticles facilitated by the aqueous *C. maxima* peel extract. The optical

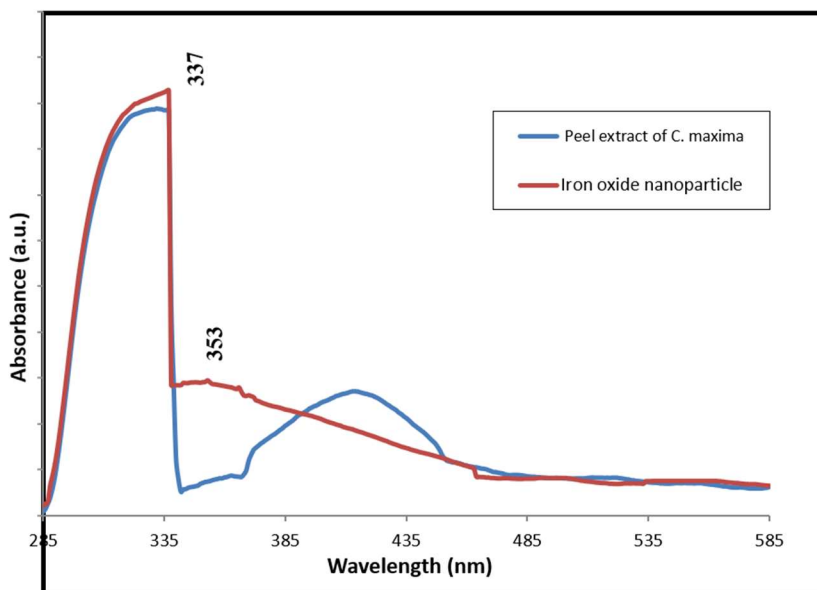
absorption spectrum of metal nanoparticles is influenced by factors such as particle size, shape, aggregation state, and the surrounding dielectric medium. Initially, the brown color is primarily attributed to the *C. maxima* peel extract, which gradually fades while undergoing magnetic stirring at 80 °C for 1 hour, resulting in a darker color as the concentration of IONPs increases. To maintain an appropriate pH for IONPs synthesis, the reaction mixture was adjusted to pH 11 using 1M NaOH, monitored by a pH meter, and confirmed by observing the absorbance of IONPs using a UV-visible spectrophotometer (Bhuiyan *et al.*, 2020; Mahlaule-Glory *et al.*, 2022; Adhikari *et al.*, 2022).

### **Analysis of Optical Properties of IONPs by UV-visible Spectroscopy**

Based on the UV-visible spectra provided in figure 2, the presence of a distinctive UV absorption peaks at 337 nm and 353 nm at pH 11 confirms the formation of IONPs. Among the various IONPs mixtures, the sharp and intense peak observed at pH 11 indicates the presence of a maximum surface plasmon resonance (SPR) band centered at 353 nm. This observation suggests the reduction of  $\text{Fe}^{+3}$  ions to  $\text{Fe}^0$  nanoparticles (Somchaidee *et al.*, 2018; Win *et al.*, 2021).

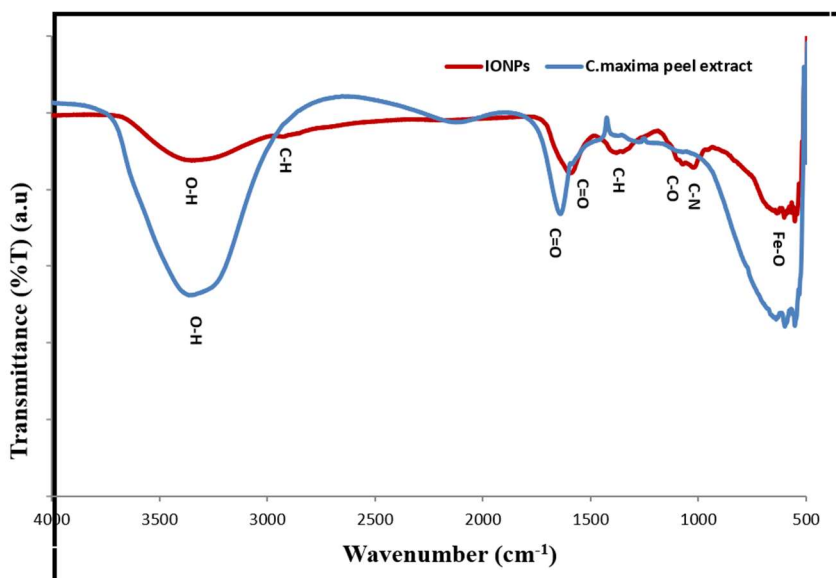
### **Figure 2**

*UV-visible Spectra of IONPs and Plant Extract*



### FTIR Analysis of *C. maxima* Peel Extract and IONPs

Fourier Transform Infrared Spectroscopy (FTIR) was utilized to detect the functional group present in the plant extract and the resulting nanoparticles. The study revealed that the reaction between phytochemical and metal ions indicated the formation of iron oxide nanoparticles. It was found that the phytochemicals reacted with the iron ions, leading to the formation of the nanoparticles, rather than reducing  $\text{Fe}^{3+}$  to  $\text{Fe}^0$ . The presence of biomolecules acting as capping agents confirmed the involvement of natural compounds in the synthesis and stability of IONPs. The FTIR analysis of the synthesized sample confirmed the synthesis of IONPs and the presence of various reducing agents, represented by the functional groups present in the *C. maxima* peel extract (Somchaidee *et al.*, 2018; Sundari *et al.*, 2017; Win *et al.*, 2021).

**Figure 3***FTIR spectra of IONPs and Plant Extract*

Polyphenols, present in the *C. maxima* peel extract as major constituents, play a significant role in the reduction of ferric ions into metallic nanoparticles due to their abundant –OH group, which release electrons to conveniently reduce  $\text{Fe}^{3+}$  to  $\text{Fe}^0$  nanoparticles upon absorption of visible light. During the reduction process, charge transfer occurs, and the initial chelation of  $\text{Fe}^{3+}$  ions by the aldehyde groups  $\text{C}=\text{O}$  in the *Citrus maxima* peel extract leads to the formation of ferric protein chain ( $\text{HO}^{\cdot}\dots\text{Fe}^{3+}\dots$ ) bonds and the subsequent formation of suspended ferric hydroxide,  $\text{Fe}(\text{OH})_3$ . Over time, the ferric hydroxide core undergoes dehydration ( $-\text{H}_2\text{O}$ ) and transforms into black-colored  $\alpha\text{-Fe}_2\text{O}_3$  nanoparticles. The protein chain in the *Citrus maxima* peel extract acts as a capping agent on the  $\alpha\text{-Fe}_2\text{O}_3$  surface through the chelation of  $\text{COO}^{\cdot}\dots\text{Fe}^{3+}$ . By adjusting the pH to 11 with the addition of 1M NaOH solution to the reaction mixture, any remaining  $\text{Fe}^{3+}$  ions that were not converted to  $\text{Fe}_2\text{O}_3$  nanoparticles

form suspended ferric hydroxide,  $\text{Fe}(\text{OH})_3$ , contributing to the formation of  $\alpha\text{-Fe}_2\text{O}_3$  (commonest form of Fe(III) oxide) nanoparticles.

The FTIR spectra of IONPs and *C. maxima* peel extract as shown in figure 3 exhibit distinct peaks corresponding to characteristic functional groups at specific wavelengths ranging from (400-4000  $\text{cm}^{-1}$ ). These functional groups existed in plant extracts act as reducing and stabilizing agents in the nanoparticle synthesis. The peaks observed at 477.28  $\text{cm}^{-1}$ , 553.11  $\text{cm}^{-1}$  and 639.95  $\text{cm}^{-1}$  indicate the presence of Fe-O bond in the sample. The peak observed at 3358.45  $\text{cm}^{-1}$  represents O-H bond stretching (H-bonded) which may be phenolic groups present in polyphenolic compounds. The peak at 2927.58  $\text{cm}^{-1}$  is due to the C-H stretching vibration present in fatty acids. Again, the stretching vibration of C=O at 1640.60  $\text{cm}^{-1}$  represents the aldehydes and ketones indicating the presence of phenolic acids and terpenoids. The C-O stretching vibration at 1277.58  $\text{cm}^{-1}$  suggests the presence of secondary alcohol in the plant extract. Likewise, the peaks observed at 1380.25  $\text{cm}^{-1}$  and 1024.07  $\text{cm}^{-1}$  represents the C-H bending vibration and C-N stretching vibration respectively indicating the presence of phenols and aliphatic amines. Therefore, the shift in peak position in the range of 400-4000  $\text{cm}^{-1}$  suggests that these functional groups containing compounds present in the plant extract are bound to the iron oxide surface (Bhuiyan *et al.*, 2020; Mahlaule-Glory *et al.*, 2022; Adhikari *et al.*, 2022).

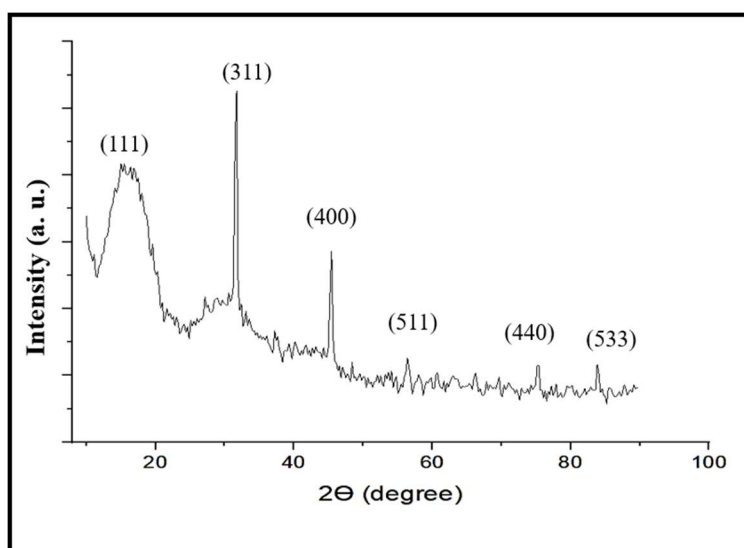
### **X-Ray Diffractometric Analysis**

The analysis of the X-ray diffraction (XRD) pattern reveals distinct peaks at specific  $2\theta$  values: 31.63°, 45.52°, 56.47°, 75.44° and 83.98° corresponding to the lattice plane values of (311), (400), (511), (440) and (533), respectively (Figure 4). These peak positions indicate the cubic crystalline structure of the synthesized IONPs, which resembles the crystals formed in the previous researches (Adhikari *et al.*, 2022; Somchaidee *et al.*, 2018). Therefore, based on

the XRD pattern, it is confirmed that the IONPs synthesized with the assistance of *C. maxima* are crystalline. These findings are consistent with previously reported results (Qasim *et al.*, 2020; Somchaidee *et al.*, 2018). Furthermore, utilizing the Scherrer equation and the full width at half maximum (FWHM) value, the average crystallite size was calculated to be 8.70 nm. In addition to these, there are additional smaller peaks observed in the XRD pattern, which could be attributed to the presence of the crystalline bio-organic phase (capping agent) on the surface of the IONPs.

**Figure 4**

*XRD Pattern of Iron Oxide Nanoparticles*



It is also possible that the characteristic peaks arise from the partial oxidation of iron, resulting in the observed features.

#### **Photocatalytic Degradation of Methylene Blue**

The methylene blue of 10 ppm concentration has intense blue color before adding IONPs and  $H_2O_2$ . After the addition of 0.2 mL  $H_2O_2$  and 10 mg of IONPs, the blue color of the MB solution fades away to some extent (Adhikari *et al.*, 2022). After 90 minutes, it became a colorless solution as shown in the figure 5.

The objective of this experiment was to assess the effectiveness of synthesized IONPs for the oxidative degradation of MB. The UV-vis spectrum of the MB solution, in the presence of IONPs and H<sub>2</sub>O<sub>2</sub>, was recorded at various time intervals while continuously stirring on a magnetic stirrer in sunlight. Small samples were taken at specific time intervals to measure the absorbance of the solution.

### Figure 5

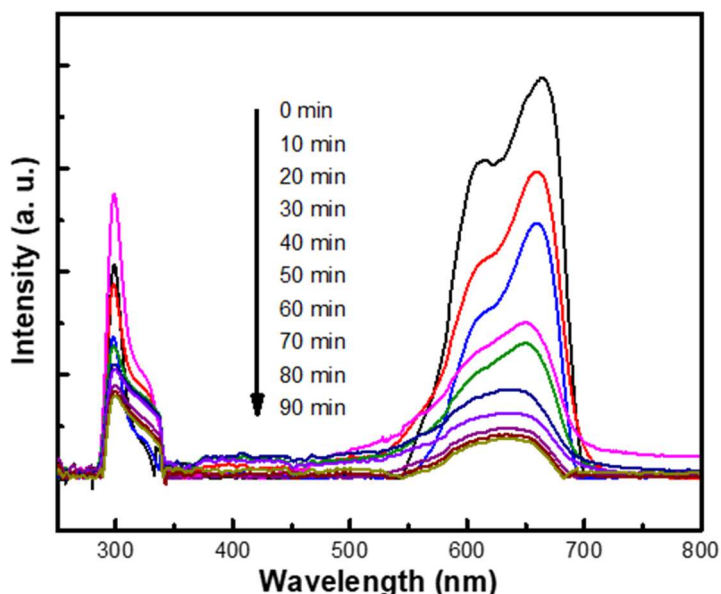
*Photographic Image of the MB Dye Degradation Photocatalytically at Different Intervals of Time by Plant-mediated Synthesized IONPs*



Initially, the SPR band of MB was observed at 663 nm with an absorbance of 0.594 nm accompanied by a hump at 620 nm, which is attributed to  $\pi \rightarrow \pi^*$  and  $n \rightarrow \pi^*$  transitions. Over time, the SPR band gradually decreased from its maximum value of 0.594 at 664 nm due to continuous exposure to sunlight, resulting in a fading of the intense blue color of MB. The decline in the SPR band of the solution, as depicted in the figure 6, continued until 1.5 hours, and eventually, the solution became colorless after 1.5 hours.

### Figure 6

*Photocatalytic Degradation of MB at Different Intervals of Time by 5 mg Dose of IONPs*

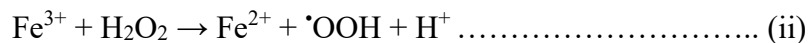


The complete degradation of methylene blue (MB) was confirmed by the UV-visible spectrophotometer, which exhibited an intense peak at 664 nm. The degradation efficiency of the dye was calculated using the following formula:

$$\text{Efficiency (\%)} = (A_0 - A_t) / A_0 \times 100$$

Where, efficiency (%) represents the degradation efficiency of the dye,  $A_0$  corresponds to the absorbance of the dye solution at the beginning (zero time), and  $A_t$  represents the absorbance of the dye solution in suspension after time  $t$ .

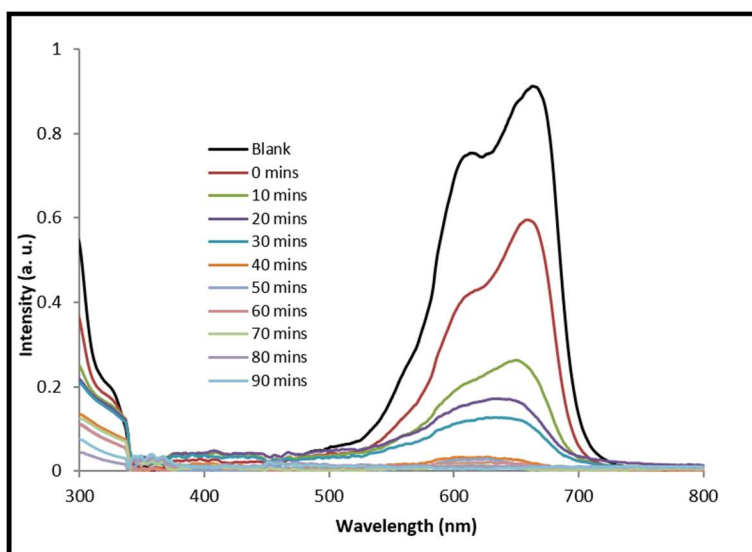
The reactions involved in the degradation process are as follows:



Equations (i) and (ii) demonstrate that the reaction is initiated by hydrogen peroxide, resulting in the generation of hydroxyl radicals that attack and degrade methylene blue (MB). These hydroxyl radicals also target the bonds in MB whether they are in solution or adsorbed on the surface of IONPs. Previous literatures (Shafreen *et al.*, 2017; Wanakai *et al.*, 2019) indicates that  $H_2O_2$  alone does not cause significant degradation. However, when IONPs are combined with  $H_2O_2$ , the color of MB disappears with an efficiency of 90.06%, 98.31% and 93.08% for 5 mg, 10 mg and 20 mg of IONPs respectively, after 90 minutes. No significant changes are observed beyond 90 minutes. Incubating MB in an aqueous solution of IONPs and  $H_2O_2$  for 5 minutes results in a red shift of the spectral band from 620 nm to 664 nm, which can be attributed to MB protonation (Shahwan *et al.*, 2011).

### Figure 7

*Photocatalytic Degradation of MB at Different Intervals of Time by 10 mg Dose of IONPs*

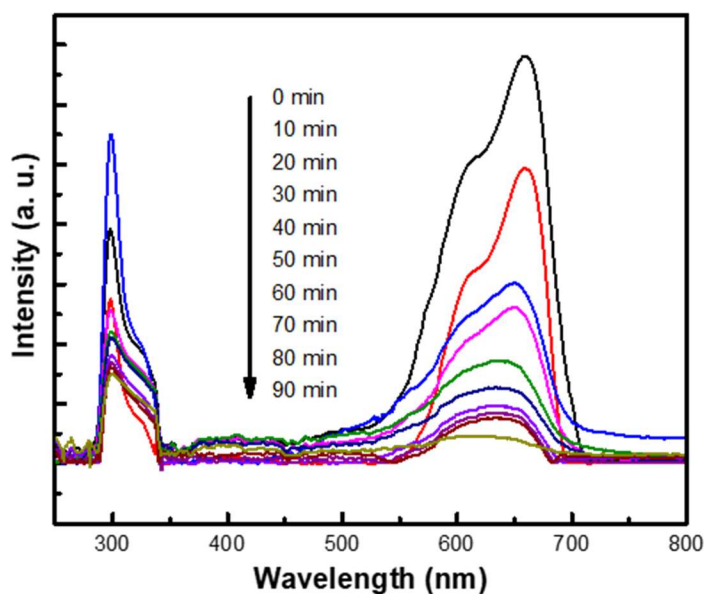


Consequently, MB undergoes oxidation and decolorization through a Fenton-like reaction, facilitated by IONPs providing ferrous ions. Similar findings

have been reported by Adhikari *et al.*, (2022), who synthesized IONPs using the sol-gel method and have demonstrated the potential of green-synthesized IONPs for organic dye degradation. Therefore, the synthesized IONPs can be utilized as heterogeneous Fenton-like oxidants for the degradation of MB in an aqueous medium.

### Figure 8

*Photocatalytic Degradation of MB at Different Intervals of Time by 20 mg Dose of IONPs*



### Degradation Kinetics of Methylene Blue

The estimation of dye photodegradation's kinetic constants is commonly done by utilizing equations that represent pseudo-first-order and second-order reaction rates (Eq. (vi) and (vii)). The equations for the reaction rate are as follows:

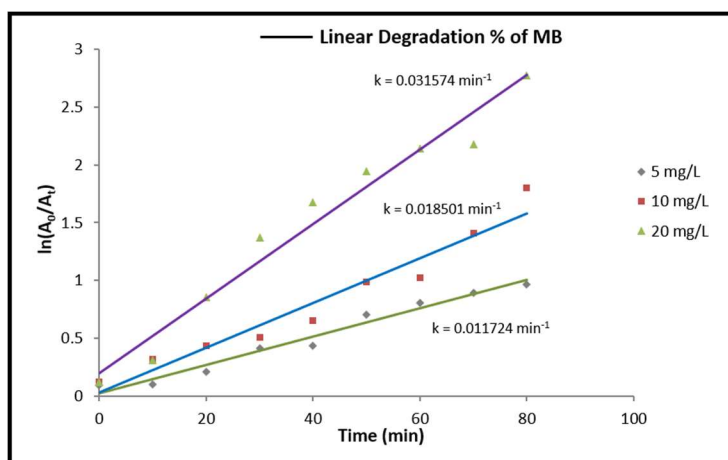
$$\ln(A_0/A_t) = K_1 t \dots\dots\dots (vi)$$

$$1/A_0 - 1/A_t = K_2 t \dots\dots\dots (vii)$$

In these equations,  $t$  represents the reaction time in minutes,  $A_0$  is the initial concentration,  $A_t$  is the concentration at time  $t$ , and  $K_1$  ( $\text{hr}^{-1}$ ) represents the first-order reaction rate constant. The rate constant ( $K$ ) of the first-order reaction is determined by plotting  $\ln(A_0/A_t)$  against the reaction time,  $t$ . The slowest degradation rate was observed at 30 minutes for a sample, with a rate constant of  $0.00634 \text{ min}^{-1}$ ,  $0.0151 \text{ min}^{-1}$  and  $0.02751 \text{ min}^{-1}$  for 5 mg, 10 mg and 20 mg of IONPs, respectively. This rate increased to  $0.01172 \text{ min}^{-1}$ ,  $0.0185 \text{ min}^{-1}$  and  $0.03157 \text{ min}^{-1}$  for 5 mg, 10 mg and 20 mg of IONPs at 90 minutes due to redox reactions occurring between IONPs (Iron Oxide Nanoparticles) and MB (Methylene Blue), resulting in the generation of oxidative free radicals that bind with photocatalysts and trap the molecules of MB, ultimately removing them from polluted water.

### Figure 9

*Rate of Degradation of Methylene Blue by Different Doses of IONPs at Different Time Intervals*

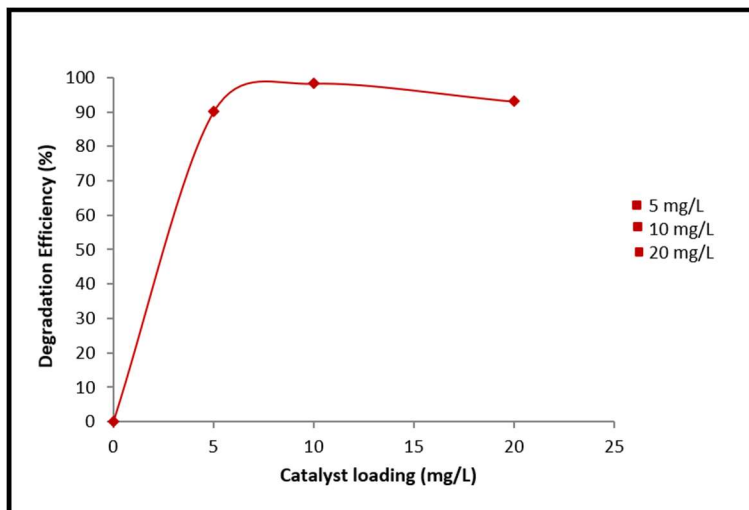


This indicates that the reaction rate is significantly higher at different time intervals with a slope of  $0.01172 \text{ min}^{-1}$ ,  $0.0185 \text{ min}^{-1}$  and  $0.03157 \text{ min}^{-1}$  for 5 mg, 10 mg and 20 mg of IONPs, respectively. The dye degradation reached half of its

initial value within 45 minutes, corresponding to a reaction rate of  $0.00922 \text{ min}^{-1}$ ,  $0.01298 \text{ min}^{-1}$  and  $0.03626 \text{ min}^{-1}$  for 5 mg, 10 mg and 20 mg of IONPs, respectively. The relative degradation kinetics of IONPs has been reported in published researches (Bhuiyan *et al.*, 2020; Adhikari *et al.*, 2022). Ultimately, within 90 minutes, 90.06%, 98.31% and 93.08% of MB dye degradation was achieved using 5 mg, 10 mg and 20 mg of IONPs which continuously produce hydroxyl radicals ( $\text{OH}^\cdot$ ) under sunlight radiation, along with  $\text{H}_2\text{O}_2$ . These compounds are responsible for the degradation of the MB dye and a probable degradation percentage is given in the figures 6, 7 and 8.

### Figure 10

*Degradation Efficiency Different Doses (5 mg, 10mg & 20 mg) of IONPs*



In general, when nanoparticles (NPs) are irradiated by sunlight, an electron ( $e^-$ ) and a hole ( $h^+$ ) pair are generated (Varadavenkatesan *et al.*, 2019). The electron is excited from the valence band to the conduction band, leaving the hole ( $H^+$ ) in the valence band. These holes are responsible for the conversion of water into hydroxyl radicals, which then oxidatively degrade the dye. On the other hand, the electron combines with molecular oxygen to form a superoxide radical. The superoxide radical further converts into a hydroxyl radical, a strong oxidizing

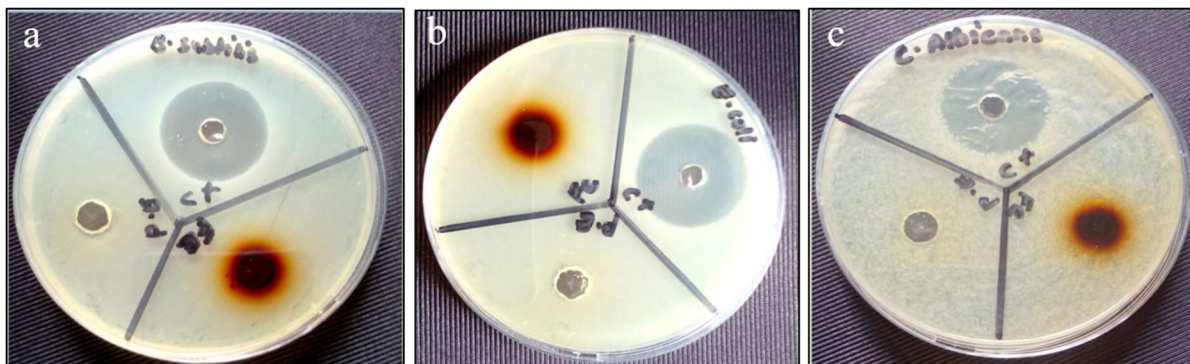
agent that degrades the dye into harmless end products (Kamaraj *et al.*, 2019). Additionally, the highly oxidizing holes generated by NPs, after absorbing sunlight, directly oxidize the dyes and release  $H^+$  ions, which then combine with water to produce reactive oxygen species and  $OH^-$  ions. These species contribute to the degradation of the dye. Furthermore, the various biomolecules present in plant extract and even in the NPs surface act like catalysts to boost the photocatalytic activity and the subsequent enriched degradation of dye molecules (Haritha *et al.*, 2016).

### **Anti-microbial Activity of IONPs**

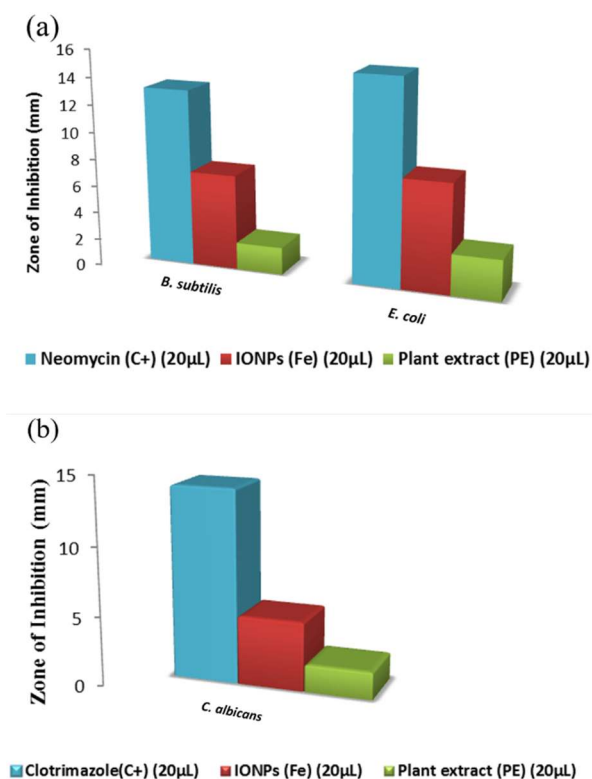
The disc diffusion method was used to investigate the antibacterial effects of IONPs against both Gram-positive (*Bacillus subtilis*) and Gram-negative (*Escherichia coli*) bacteria. The IONPs synthesized through biosynthesis exhibited superior antibacterial activity, as evidenced by larger zones of inhibition, against *B. subtilis* and *E. coli*. A comparison between *B. subtilis* and *E. coli* demonstrated that the green-synthesized IONPs displayed effective antibacterial activity, with a zone of inhibition measuring 15 mm for *B. subtilis* and 7 mm for *E. coli* (Figure 11 and 12). These findings suggest that the biosynthesized IONPs can convert dissolved oxygen molecules into superoxide radical anions ( $O_2^-$ ) (Das *et al.*, 2020; Ismail *et al.*, 2015), resulting in the production of free radicals such as  $\cdot O_2$  and  $OH^-$ . These radicals can depolymerize polysaccharides, induce DNA strand breaks, initiate lipid peroxidation, and deactivate enzymes, ultimately leading to cell death. Additionally, it is plausible that the interaction between nanoparticles and cell membrane proteins through electrostatic interactions, as well as the accumulation of nanoparticles in the cytoplasm or periplasmic region, disrupts cellular function and causes membrane disruption and disorganization (Rufus *et al.*, 2016).

**Figure 11**

*Antimicrobial Performance of IONPs against the bacterial strains: (a) B. Subtilis, (b) E. coli, and (c) fungal strain C. albicans*



The antifungal activity of IONPs against *Candida albicans* was evaluated using the Agar Well Disc Diffusion method. The green-synthesized IONPs exhibited notable antifungal activity against *C. albicans*, with a zone of inhibition measuring 6 mm (Figure 11 and 12). These findings align with previously published results (Seddighi *et al.*, 2017). Previous research has proposed two possible mechanisms for the interaction between nanoparticles and bacteria/fungi. One mechanism involves the increased production of reactive oxygen species (ROS) such as hydroxyl radicals ( $\cdot\text{OH}$ ), singlet oxygen ( $\cdot\text{O}_2$ ), and hydrogen peroxide ( $\text{H}_2\text{O}_2$ ) (Caldeiro *et al.*, 2021). When IONPs with defects are activated by UV or visible light, electron-hole pairs are formed. The resulting holes can split  $\text{H}_2\text{O}$  molecules into  $\text{OH}^-$  and  $\text{H}^+$ . Additionally, the addition of electrons converts dissolved oxygen molecules into superoxide radical anions ( $\text{O}_2^-$ ). These free radicals are consistent with results reported elsewhere (Das *et al.*, 2020; Rufus *et al.*, 2016).

**Figure 12***Effectiveness of IONPs against Microbes in Comparison to Antibiotic Controls*

The anti-microbial activity of synthesized IONPs was carried out at Himalaya Research Institute of Biotechnology Pvt. Ltd., Srijananagar, Bhaktapur, Nepal.

### Conclusions

Green synthesis of iron oxide nanoparticles using *C. maxima* peel extract was completed and confirmed by the color change and surface plasmon resonance (SPR) spectra of the solution. The maximum absorption peaks were in the range of 337 and 353 nm in the UV-vis spectra. It was affirmed that the *C. maxima* peel extract has the special property to reduce  $\text{Fe}^{+3}$  ion to  $\text{Fe}^0$ , the IONPs, and the average size of IONPs was calculated to be 8.70 nm from the most intense XRD peak using Scherrer's equation. FTIR spectra of the as-synthesized IONPs assured

that the reducing and capping agents are polyphenolic compounds present in the extract.

The as-synthesized IONPs were found to play a vital role in the degradation of harmful organic dyes like methylene blue from polluted water photocatalytically in 90 minutes with 90.06%, 98.31% and 93.08% efficiency by the dose of 5 mg, 10 mg and 20 mg of IONPs per 100 mL of 10 ppm dye solution, respectively. Such results can be crucial in the field of industry for commercial use. Likewise, in vitro study of the IONPs also demonstrated good anti-bacterial activity against *Bacillus subtilis* and *Escherichia coli* and good anti-fungal activity in vitro against *Candida albicans* demonstrating the possibility for topical administration against these bacterial and fungal infections. Furthermore, the green synthesis of IONPs using peels of *C. maxima* may be helpful in the field of nanotechnology which has a potential contribution to the field of research and the protection of the environment.

### References

- Adhikari, A., Chhetri, K., Acharya D., Pant, B., & Adhikari, A. (2022). Green synthesis of iron oxide nanoparticles using *Psidium guajava* L. leaves extract for degradation of organic dyes and anti-microbial applications. *Catalysts*, *12*, 1188.
- Ahammed, K.R., Ashaduzzaman, M., Paul, S.C. (2020). Microwave assisted synthesis of zinc oxide (ZnO) nanoparticles in a noble approach: Utilization for antibacterial and photocatalytic activity. *SN Applied Sciences*, *2*, 955.
- Ahmed, S., Saifullah, Ahmad, M., Swami, B. L., & Ikram, S. (2016). Green synthesis of silver nanoparticles using *Azadirachta indica* aqueous leaf extract. *Journal of Radiation Research and Applied Sciences*, *9*(1), 1–7.
- Anchan, S., Pai, S., Sridevi, H., Varadavenkatesan, T., Vinayagam, R., & Selvaraj, R. (2019). Biogenic synthesis of ferric oxide nanoparticles using the leaf extract of *Peltophorum pterocarpum* and their catalytic dye degradation potential. *Biocatalysis and Agricultural Biotechnology*, *20*, 101251.
- Bhuiyan, M.S.H., Miah, M.Y., Paul, S.C., Das, T. Aka., Saha, O., Rahaman, M.M., Sharif, M.J.I., Habiba, O., & Ashaduzzaman, M. (2020). Green synthesis of iron Oxide nanoparticle using *Carica papaya* leaf extract: Application for photocatalytic degradation of remazol yellow RR dye and antibacterial activity. *Heliyon*, *6*(8).
- Bibi, I., Nazar, N., Ata, S., Sultan, M., Ali, A., Abbas, A., Jilani, K., Kamal, S., Sarim, F.M., Khan, M.I., Jalal, F., & Iqbal, M. (2019). Green synthesis of iron oxide nanoparticles using pomegranate seeds extract and photocatalytic activity evaluation for the degradation of textile dye. *Journal of Materials Research and Technology*, *8*, 6115–6124.

- Caldeirão, A.C.M., Araujo, H.C., Tomasella, C.M., Sampaio, C., dos Santos Oliveira, M.J., Ramage, G., Pessan, J.P., & Monteiro, D.R. (2021). Effects of antifungal carriers based on chitosan-coated iron oxide nanoparticles on microcosm biofilms. *Antibiotics*, *10*, 588.
- Das, S., Diyali, S., Vinothini, G., Perumalsamy, B., Balakrishnan, G., Ramasamy, T., Dharumadurai, D., & Biswas, B. (2020). Synthesis, morphological analysis, antibacterial activity of iron oxide nanoparticles and the cytotoxic effect on lung cancer cell line. *Heliyon*, *6*(9).
- Haritha, E., Roopan, S.M., Madhavi, G., Elango, G., Al-Dhabi, N.A., Arasu, M.V. (2016). Green chemical approach towards the synthesis of SnO<sub>2</sub> NPs in argument with photocatalytic degradation of diazo dye and its kinetic studies. *Journal of Photochemistry and Photobiology*, *162*, 441–447.
- Izadiyan, Z., Shameli, K., Miyake, M., Hara, H., Mohamad, S.E.B., Kalantari, K., Taib, S.H.M., & Rasouli, E. (2020). Cytotoxicity assay of plant-mediated synthesized Iron oxide nanoparticles using *Juglans regia* green husk extract. *Arabian Journal of Chemistry*, *13*(1), 2011-2023.
- Jamzad, M., & Kamari, B. M. (2020). Green synthesis of iron oxide nanoparticles by the aqueous extract of *Laurus nobilis* L. leaves and evaluation of the antimicrobial activity. *Journal of Nanostructure in Chemistry*, *10*, 193–201.
- Kamaraj, M., Kidane, T., Muluken, K.U., Aravind, J. (2019). Biofabrication of iron oxide nanoparticles as a potential photocatalyst for dye degradation with antimicrobial activity. *International Journal of Environmental Science and Technology*, *16*(5), 8305–8314.
- Kirdat, P. N., Dandge, P.B., Hagwane, R.M., Nikam, A.S., Mahadik, S.P., & Jirange, S.T. (2021). Synthesis and characterization of ginger (*Z. officinale*) extract mediated iron oxide nanoparticles and its antibacterial activity. *Materials Today: Proceedings*, *43*, 2826-2831.

- Kumar, B.; Kumari, S.; Galeasc, S.; Sharmad, V.; Guerreroc, V. H.; Debuta, A.; Cumbala, L. (2020). Characterization and application of biosynthesized iron oxide Nanoparticles using *Citrus paradisi* peel: A sustainable approach. *Inorganic Chemistry Communications*, 119, 108116.
- Mahlaule-Glory, L. M., Mapetla, S., Makofane, A., Mathipa, M. M., & Hintsho-Mbita, N.C. (2022). Biosynthesis of iron oxide nanoparticles for the degradation of methylene blue dye, sulfisoxazole antibiotic and removal of bacteria from real water. *Heliyon*, 8(9).
- Qasim, S., Zafara, A., Muhammad Saqib, S., Alib, Z., Nazara, M., Muhammad W., Ul-Haqa, A., Tariqa, T., Hassand, S. G., Iqbalc, F., Shue, X-Gang., & Hasana, M. (2020). Green synthesis of iron oxide nanorods using *Withania coagulans* extract improved photocatalytic degradation and antimicrobial activity. *Journal of Photochemistry & Photobiology B: Biology*, 204, 111784.
- Rufus, A., Sreeju, N., & Philip, D. (2016). Synthesis of biogenic hematite ( $\alpha$ -Fe<sub>2</sub>O<sub>3</sub>) nanoparticles for antibacterial and nanofluid applications. *RSC Advances*, 6, 94206– 94217.
- Sapkota, K.P., Lee, I., Hanif, M.A., Islam, M.A., & Hahn, J.R. (2019). Solar-light-driven efficient ZnO–single-walled carbon nanotube photocatalyst for the degradation of a persistent water pollutant organic dye. *Catalysts*, 9 (6), 498.
- Shafreen, R.B., Seema, S., Ahamed, A.P., Thajuddin, N., & Alharbi, S.A. (2017). Inhibitory effect of biosynthesized silver nanoparticles from extract of *Nitzschia palea* against curl-mediated biofilm of *Escherichia coli*. *Applied Biochemistry and Biotechnology*, 183, 1351-1361.
- Shahwan, T., Abu Sirriah, S., Nairat, M., Boyac, E., Eroglu, A.E., Scott, T.B., & Hallam, K.R. (2011). Green synthesis of iron nanoparticles and their

- application as a fenton-like catalyst for the degradation of aqueous cationic and anionic dyes. *Chemical Engineering Journal*, 172, 258–266.
- Somchaidee, P., & Tedsree, K. (2018). Green synthesis of high dispersion and narrow size distribution of zero-valent iron nanoparticles using guava leaf (*Psidium guajava* L.) extract. *Advances in Natural Sciences: Nanoscience and Nanotechnology*, 9, 035006.
- Sundari, J.J., Praba, P., Brightson, Y., Brightson Arul Jacob, Y., Vasantha, V., Shanmugaiah, V. (2017). Green synthesis and characterization of zero valent iron nanoparticles from the leaf extract of *Psidium guajava* plant and their antibacterial activity. *Chemical Science Review and Letters*, 6(22), 1244–1252.
- Varadavenkatesan, T., Lyubchik, E., Pai, S., Pugazhendhi, A., Vinayagam, R., Selvaraj, R., (2019). Photocatalytic degradation of Rhodamine B by zinc oxide nanoparticles synthesized using the leaf extract of *Cyanometra ramiflora*. *Journal of Photochemistry and Photobiology B: Biology*, 199, 111621.
- Wanakai, S. I., Kareru, P. G., Makhanu, D. S., Madivoli, E. S., Maina, E. G., & Nyabola, A. O. (2019). Catalytic degradation of methylene blue by iron nanoparticles synthesized using *Galinsoga parviflora*, *Conyza bonariensis* and *Bidens pilosa* leaf extracts. *SN Applied Sciences*, 1, 1-10.
- Win, T.T., Khan, S., Bo, B., Zada, S. & Fu, P. (2021). Green synthesis and characterization of Fe<sub>3</sub>O<sub>4</sub> nanoparticles using chlorella-K01 extract for potential enhancement of plant growth stimulating and antifungal activity. *Scientific Reports*, 11, 21996.
- Zou, Z., Xi, W., Hu, Y., Nie, C., Zhou, Z. (2016). Antioxidant activity of *Citrus* fruits. *Food Chemistry*, 196, 885-896.